Journal of the Serbian Chemical Society
JSCS-info@shd.org.rs • www.shd.org.rs/JSCS
J. Serb. Chem. Soc. 79 (8) 977–991 (2014)
JSCS–4641
UDC 667.281+66.094.3+546.72'824–31+54–732:621.021.1/.4
Original scientific paper

Fenton-like oxidation of an azo dye using mesoporous Fe/TiO_2 catalysts prepared by a microwave-assisted hydrothermal process

JELENA NEŠIĆ[1*#], DRAGAN D. MANOJLOVIĆ[2#], MILICA JOVIĆ[1#], BILJANA P. DOJČINOVIĆ[3], PREDRAG J. VULIĆ[4], JUGOSLAV KRSTIĆ[5] and GORAN M. ROGLIĆ[2**#]

[1]Innovation Center of the Faculty of Chemistry, University of Belgrade, Studentski trg 12, 11000 Belgrade, Serbia, [2]Faculty of Chemistry, University of Belgrade, Studentski trg 12, Belgrade, Serbia, [3]Institute of Chemistry, Technology and Metallurgy, Center of Chemistry, University of Belgrade, Njegoševa 12, 11000 Belgrade, Serbia, [4]Laboratory of Crystallography, Faculty of Mining and Geology, University of Belgrade, Đušina 7, 11000 Belgrade, Serbia and [5]Institute of Chemistry, Technology and Metallurgy, Department of Catalysis and Chemical Engineering, University of Belgrade, Njegoševa 12, 11000 Belgrade, Serbia

(Received 1 October, revised 20 November, accepted 21 November 2013)

Abstract: Fe-doped TiO_2 photocatalysts with different contents of Fe (0.5, 1.6, 3.4 and 6.4 %) were synthesized by a microwave-hydrothermal method and characterized by X-ray diffraction analysis, N_2 physisorption at 77 K and UV–Vis spectrometry. The characterization showed that the Fe ions were highly dispersed in the TiO_2 lattice. It was found that all the synthesized catalysts had a mesoporous structure and that Fe-doping increased the BET surface area. The UV–Vis study showed that the absorption spectra were shifted to longer wavelengths (red shift) with increasing dopant concentration. The photocatalytic activity of the samples was evaluated by the decolorization of the textile dye Reactive Blue 52 (RB) in aqueous solutions under sun-like radiation in the presence of H_2O_2 (a heterogeneous photo-Fenton process). The photocatalyst with 3.4 % Fe was found to be the most efficient in the presence of H_2O_2. The effect of the initial pH of the dye solution was assessed and dissolution of iron ions was studied as a function of pH value. It was concluded that decolorization was more favorable in acidic pH, and that at pH values >4, the release of Fe ions into the solution was negligible. Photocatalytic degradation of 4-chlorophenol (4-CP) was investigated under the optimal conditions and it was shown that the catalyst was capable of degrading colorless pollutants.

Keywords: Fe/TiO_2; heterogeneous photo-Fenton; Reactive Blue 52; 4-chlorophenol.

Corresponding authors. E-mail: (*)jelenanesic@chem.bg.ac.rs; (**)groglic@chem.bg.ac.rs
[#] Serbian Chemical Society member.
doi: 10.2298/JSC131001143N

INTRODUCTION

Dye pollution from textile plants is a source of environmental concern the world over. These effluents are toxic and mostly non-biodegradable. Moreover, they absorb and scatter sunlight and thus, affect aquatic ecosystems. Most of the dye molecules are resistant to destruction by conventional methods for water treatment (coagulation, carbon adsorption, reverse osmosis, ultrafiltration and biological treatments).[1] In the last decades, advanced oxidation processes (AOPs) appear to be a promising alternative for the degradation of organic pollutants. These processes are based on the generation of very reactive species, such as hydroxyl ($^{\bullet}OH$) and hydroperoxyl ($HO_2^{\bullet}$) radicals, and complete mineralization of the target pollutant species is achieved.[2]

Among the advanced oxidation processes, titanium dioxide (TiO_2) offers a great potential as a photocatalytic material for detoxifying wastewater. TiO_2 has the advantage of being non-toxic and stable in aqueous solutions. Furthermore, photo-assisted processes are inexpensive and do not require special conditions. They are open-atmospheric systems that can operate at room temperature, utilizing natural solar light as an energy source.

In addition, the photo-Fenton oxidation is a very efficient system for the degradation of pollutants. This method involves the catalytic decomposition of H_2O_2 in the presence of ferrous ions, resulting in the generation of hydroxyl radicals. The formation of hydroxyl radicals and the regeneration of Fe^{2+} by photo-reduction from Fe^{3+} can be represented by the following reactions:[3]

$$Fe^{2+} + H_2O_2 \rightarrow Fe(OH)^{2+} + {}^{\bullet}OH \quad (1)$$

$$Fe(OH)^{2+} + h\nu \rightarrow Fe^{2+} + {}^{\bullet}OH \quad (2)$$

Both of these processes suffer from limitations. TiO_2 has wide bandgap (3.2 eV), which means it can utilize only ≈5 % of the solar spectrum, all in the UV region.[4] This problem is partially overcome by doping with different species, such as: iron,[5–7] nitrogen–sulfur,[8] silver,[9,10] molybdenum[11] and lanthanum,[12] which enables the reactions to be induced not only with UV, but also with visible light. The homogenous photo-Fenton system requires a pH of ≈3, in order to avoid the formation of insoluble $Fe(OH)_3$, and the after treatment separation of the dissolved iron ions.[13]

In order to overcome these problems, a combination of these two processes could be used and the advantage of potential synergistic effects taken. A heterogeneous catalyst of this type would enable operation over a wide pH range, a TiO_2 and Fenton reagent combination would enhance visible-light absorption and the removal of sludge containing Fe ions would not be necessary, which would reduce the costs of treatment.[14,15]

The aim of this research was to prepare Fe/TiO_2 materials with different contents of Fe by a microwave-assisted, hydrothermal method and investigate

their applicability as heterogeneous photo-Fenton catalysts for the decolorization of the textile dye Reactive Blue 52 (RB) in aqueous solutions under sun-like radiation in the presence of H_2O_2. The effects of different Fe contents and initial pH values of the dye solution on the decolorization efficiency were assessed. The dissolution of iron ions was studied in dependence on the experimental conditions, because it is a common phenomenon during heterogeneous photo-Fenton oxidation, which increases the contribution of the homogeneous photo-Fenton process. In addition, the degradation of 4-chlorophenol (4-CP) was investigated to show that the studied catalyst was also able to degrade colorless pollutants and that the excitation of the dye molecule is not the only mechanism, but also the production of reactive oxygen species is operative.

EXPERIMENTAL

Materials

Titanium tetrachloride, $TiCl_4$ (Fluka 98 %), ammonium hydroxide, NH_4OH (Sigma–Aldrich 25 %), iron(III) chloride, $FeCl_3$ (Merck), hydrogen peroxide, H_2O_2 (Sigma–Aldrich 30%) and 4-chlorophenol (Sigma–Aldrich) were used as received. The azo dye Reactive Blue 52 (RB) was obtained from Clariant (Switzerland) and used without further purification; the molecular structure of RB is shown in Fig. 1. All solutions were prepared with deionized water.

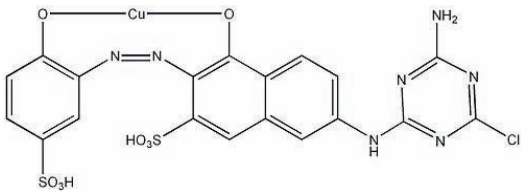

Fig. 1. Structural formula of Reactive Blue 52.

Preparation of catalysts

All the catalysts were prepared using the microwave-hydrothermal method. $TiCl_4$ was added to icy water containing the required amount of the iron salt ($TiCl_4$:H_2O (*V*/*V*) ratio 1:10) Then, the precipitation was induced by the slow addition of NH_4OH (25 %) solution under constant stirring at room temperature until the reaction mixture attained a pH between 7 and 8. The suspension was transferred into a Teflon® microwave closed vessels (digestion system ETHOS One Milestone, equipped with a High Pressure Rotor SK-10, Italy), sealed and heated by microwave irradiation, whereby the maximum temperature of 150 °C was attained in 10 min, and then kept at this temperature for a further 15 min more for hydrothermal treatment. The resulting product was separated by centrifugation and washed repeatedly with deionized water until the precipitate becomes free of chloride ion (confirmed by the $AgNO_3$ test). Finally, it was dried at 80 °C for 5 h and then calcined at 500 °C for 10 h.

Characterization

The content of Fe in the synthesized samples was determined by the inductively coupled plasma–optical emission spectroscopy (ICP–OES) technique (Thermo Scientific iCAP 6500 Duo ICP spectrometer, UK). Samples were prepared by microwave digestion using an Ethos

One microwave system (Advanced Microwave Digestion System, Milestone, Italy). Each sample (0.1 g) was mixed with 5 mL of sulfuric acid (H_2SO_4, 98 %), 2 mL of nitric acid (HNO_3, 65 %) and 1 mL of hydrofluoric acid (HF, 50 %), all analytical grade reagents from Carlo Erba, transferred into a microwave digestion vessel and microwave heated. The maximum temperature of 220 °C was reached after 15 min and then this temperature kept constant for a further 20 min. The concentrations of Fe in the prepared powders are expressed in terms of mass weight percent.

Powder X-ray diffraction (XRPD) analysis was used for the identification of the crystalline phases, a quantitative phase analysis and an estimation of the crystallite size and strain. The XRPD patterns were collected on a Philips diffractometer (PW1710) employing $CuK_{\alpha 1,2}$ radiation. Step scanning was performed within the 2θ range from 20 to 100° with a step size of 0.080° and a fixed counting time of 5 s per step. The XRPD patterns were used to refine crystallographic structure and microstructural parameters using the procedure implemented in the FullProf computer program.[16]

Adsorption–desorption isotherms were obtained by nitrogen adsorption at 77 K using a Sorptomatic 1990 Thermo Finnigan device. Prior to adsorption, the samples were outgassed for 1 h at room temperature under vacuum and additionally for 16 h at 110 °C at the same residual pressure. The specific surface areas of the samples (S_{BET}) were calculated by applying the Brunauer–Emmet–Teller (BET) Equation, from the linear part of the adsorption isotherm.[17] The total pore volumes (V_{tot}) were obtained from the N_2 adsorption, expressed in liquid form, by application of the Gurvitsch rule.[18] The micropore volumes (V_{mic}) were estimated according to the Dubinin–Radushkevich method.[19] The mesopore volumes (V_{mes}) were estimated according to the Barrett, Joyner and Halenda method from the desorption branch of the isotherms.[20]

The UV–Vis diffuse reflectance spectra (DRS) were recorded on an Evolution 600 UV––Vis spectrophotometer (Thermo Scientific), equipped with a DRA-EV-600 diffuse reflectance accessory.

Photodegradation procedure

A typical photocatalytic experiment was performed in a cylindrical photochemical reactor, with a water circulation arrangement to maintain the temperature in the range 22±1 °C. An Osram Ultra-Vitalux lamp (300 W) with a sun-like radiation spectrum was used as the light source. The distance between the lamp and the sample was 25 cm. Appropriate amounts of Fe/TiO_2 were added into 100 mL of RB solution and stirred in the dark for 1 h before illumination, to ensure the establishment of the adsorption–desorption equilibrium between the photocatalyst and RB. The pH was adjusted by the addition of H_2SO_4 or NaOH using a pH monitor (Microcomputer pH-vision 6071, JENCO Electronics Ltd., Taiwan). Concentration changes of the RB were monitored according to the decreasing intensity of the absorption peak at 615 nm. Absorption spectra of RB were recorded on a double-beam UV–Vis spectrophotometer (Cintra 10 UV–Visible spectrometer, Australia), at a fixed slit width (1 nm), using 1 cm quartz cell. The decolorization efficiency was calculated from the relation:

$$\text{Decolorization} = \frac{(A_0 - A)}{A_0} \times 100$$

where A_0 and A are the absorbance at the maximum absorption wavelength (λ_{max}) of the initial dye solution and after the treatment, respectively.

Degradation of 4-chlorophenol was monitored by high-performance liquid chromatography with photodiode array detection (HPLC-DAD). The HPLC analysis was performed

using Dionex UltiMate 3000 chromatograph. A Hypersil Gold C8 column (150 mm×3 mm, 3 μm) at 40 °C was used. The mobile phases were water as component A and acetonitrile as component B (both HPLC grade, Sigma–Aldrich). The compounds were eluted at flow rate of 1.0 ml min^{-1}. The injection volume was 10 μl and the detector was set at 280 nm. The gradient elution was as follows: 30–80 % B in 20 min. The data analyses were realized using a computer equipped with the Chromeleon 6.8 program (ThermoFisher Scientific, Bremen, Germany).

RESULTS AND DISCUSSION

X-Ray diffraction analysis of photocatalysts

The diffraction patterns of four Fe/TiO_2 catalysts are shown in Fig. 2. It can be seen that only the anatase phase (JCPDS card 78-2486) was present up to a Fe content of 6.4 %, when the presence of broad low-intensity diffraction peak at $2\theta \approx 32.5°$ for $6.4Fe/TiO_2$ could be ascribed to the pseudobrookite (Fe_2TiO_5) phase (JCPDS card 29-1360). The pseudobrookite content in this sample was determined to be 3 %. This is formed because Fe^{3+} substitute Ti^{4+} in the TiO_2 lattice. This can occur because the radii of Ti^{4+} and Fe^{3+} are similar (0.69 and

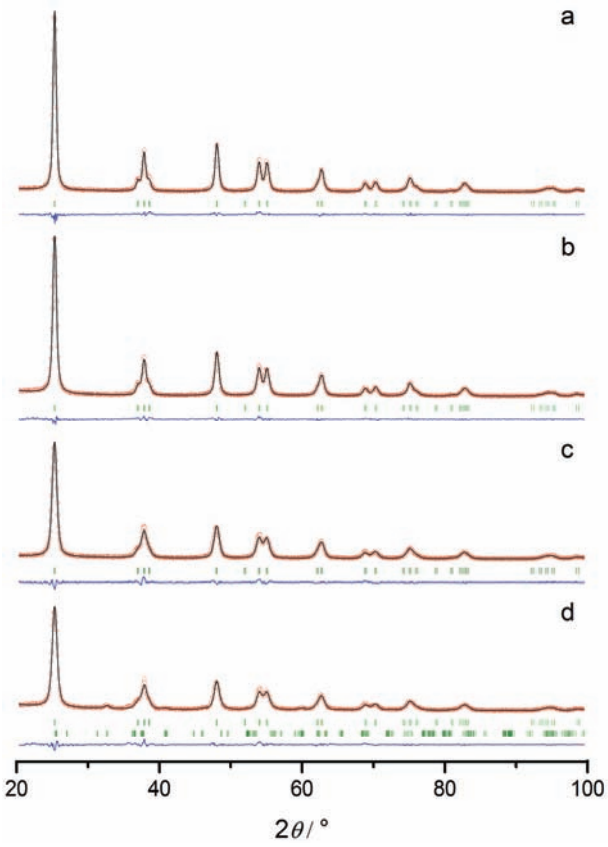

Fig. 2. The final Rietveld refinement plots of the samples: a) $0.5Fe/TiO_2$; b) $1.6Fe/TiO_2$; c) $3.4Fe/TiO_2$; d) $6.4Fe/TiO_2$. The observed data are represented by circles and the calculated data by a continuous line. The Bragg positions are denoted by vertical ticks and the difference curve is shown at the bottom.

0.64 nm for Ti^{4+} and Fe^{3+}, respectively[21]) and the electronegativities of both ions are reasonably close (Fe^{3+}: 1.96,[21] Ti^{4+}: 1.5[22]). No peaks due to Fe-oxide phase were observed in any of the samples; the Fe^{3+} were highly dispersed in the TiO_2 lattice.

Structure refinements were performed by the Rietveld method. The final Rietveld refinement plots of the samples are presented in Fig. 2, while the main results of the refinement are listed in Table I. The obtained values for the unit cell parameters of anatase show that the value of the parameter *a* varied around its reference value (a_0 = 3.78479(3) Å), while the value of the *c* parameter was slightly smaller than the reference one (c_0 = 9.51237(12) Å) in all the samples. The obtained average crystallite size slightly decreased with increasing content of Fe. The radius of the Fe^{3+} is smaller than that of Ti^{4+}; hence, the doping of Fe made the cell parameter smaller than that of pure anatase.[23]

Low values of agreement factors between the model, both structure and microstructure, and XRD data (Table I) indicate the high accuracy of the obtained results.

TABLE I. The results of the Rietveld analyses of the anatase phase (unit cell parameters, microstructure parameters and refinement residuals)

Sample	Unit cell parameters		Microstructure parameters		Rietveld refinement residuals				
	a / Å	*c* / Å	Average size Å	Average strain×10^{-3}	R_p	R_{wp}	R_{exp}	χ^2	R_B
0.5Fe/TiO_2	3.7854(2)	9.5049(6)	163	20	7.5	9.9	8.5	1.37	2.77
1.6Fe/TiO_2	3.7858(2)	9.5039(7)	128	16	7.4	9.9	8.4	1.39	1.95
3.4Fe/TiO_2	3.7884(3)	9.5040(10)	97	15	8.9	11.1	8.9	1.54	2.58
6.4Fe/TiO_2	3.7881(4)	9.4958(13)	94	15	9.7	12.1	9.3	1.69	2.34

Nitrogen physisorption

Information about specific surface areas and the pore volumes of the catalysts are summarized in Table II. The isotherms of all the synthesized materials presented in Fig. 3 could be interpreted[24] as type IV, which is typical for mesoporous materials, with an H2-type hysteresis loop, indicating the presence of pore networks. It could be seen that the position of the condensation branches on the pressure axis, the specific surface area and the pore volume were dependent on the Fe content. The introduction of the Fe ions causes an increase in specific surface area and a decrease in the pore volume. The origin of increase in the specific surface area could be explained in two ways: the reorganization of the pore system through the entrance of small particles into the pore system or the formation of a new phase, which has a higher specific surface area. The reorganization of the pore would also lead to preservation or reduction of the pore volume. From the results for V_{mic}, V_{meso} and V_{tot} given in Table II, it is clear this is

the case for synthesized Fe/TiO_2 catalysts. Fe species are not located on the outer side of the TiO_2 particles as a separate oxide phase. This statement was also confirmed by the XRD results, that Fe ions are highly dispersed in the TiO_2 lattice.

TABLE II. Textural and structural properties of the Fe/TiO_2 samples

Sample	Content of Fe, mass %	S_{BET} / m^2 g^{-1}	V_{tot} / cm^3 g^{-1}	V_{mic} / cm^3 g^{-1}	V_{meso} / cm^3 g^{-1}
0.5Fe/TiO_2	0.47	72.4	0.252	0.021	0.2189
1.6Fe/TiO_2	1.60	93.5	0.261	0.027	0.232
3.4Fe/TiO_2	3.42	83.7	0.250	0.028	0.191
6.4Fe/TiO_2	6.41	123.1	0.257	0.037	0.189

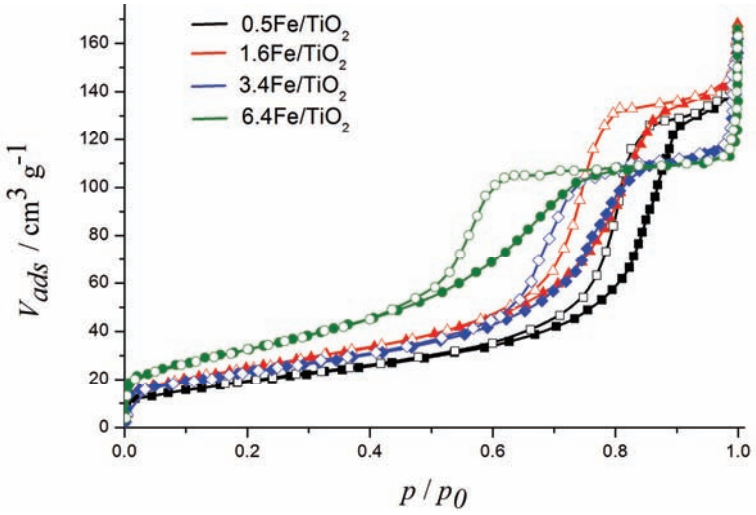

Fig. 3. Nitrogen physisorption isotherms of Fe/TiO_2 at 77 K. The empty symbols represent adsorption points and the filled symbols represent desorption points.

UV–Vis diffuse reflectance spectra

The UV–Vis diffuse reflectance spectra of synthesized samples are shown in Fig. 4. It could be seen that with increasing Fe content, the photocatalyst response shifted to higher wavelengths, which was accompanied by changes in color from pale yellow to reddish brown. The absorptions in the visible region may be induced by two factors. One is the excitation of 3d electrons of Fe^{3+} to the TiO_2 conduction band (charge transfer transition) at 415 nm.[25] The other can be ascribed to the d–d transitions $^2T_{2g} \rightarrow {}^2A_{2g}$ and $^2T_{1g}$ of Fe^{3+} or to the charge transfer transition between iron ions ($Fe^{3+} + Fe^{3+} \rightarrow Fe^{4+} + Fe^{2+}$) at 500 nm.[26,27] These results are in agreement with the XRD and nitrogen physisorption results and confirmed that the Fe ions were incorporated into the lattice of TiO_2, thus altering its crystal and electronic structures.

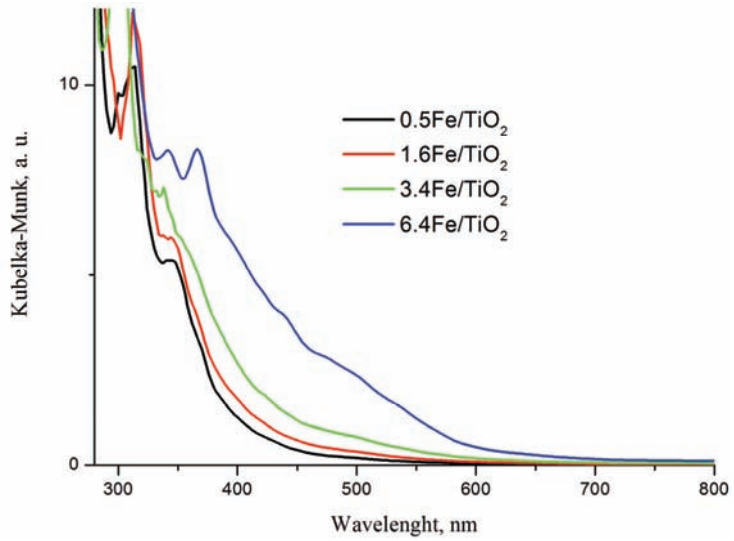

Fig. 4. Diffuse reflectance spectra of Fe/TiO_2 powders, plotted as the Kubelka–Munk function (*F*) of the reflectance (R).

Decolorization of RB

The efficiencies of different AOPs in the degradation of RB are shown in Fig. 5, from which it could be seen that the efficiency of direct photolysis under sun-like irradiation was very small. The dye removal efficiency with only H_2O_2 was much higher when H_2O_2 was applied in combination with illumination. This could be explained by the generation of highly reactive $^{\bullet}OH$ by direct photolysis of the added H_2O_2.[28] As the photolysis wavelength range of H_2O_2 is between 200 and 350 nm and since the employed lamp is active in the UV-B and UV-A regions, this reaction was possible.

In order to examine whether the presence of Fe in the Fe/TiO_2 samples influences the efficiency of photocatalytic degradation of RB, the efficiency of $3.4Fe/TiO_2$ was compared with that of the pure TiO_2. The degradation efficiency of $3.4Fe/TiO_2$ was higher, which indicates that the addition of Fe contributes to the catalytic activity. The beneficial effect of Fe ions could be explained by considering the efficient separation of the photo-excited electrons and holes.[29] Since the energy level for Fe^{3+}/Fe^{4+} is above the valence band edge of anatase TiO_2, Fe^{3+} could act as photogenerated hole traps (Eq.(3)). Fe^{3+} could also serve as photogenerated electron traps, as the energy level for Fe^{3+}/Fe^{2+} is below the conduction band edge of TiO_2 (Eq. (4)). Thus, Fe^{3+} could act as both electron and hole traps, whereby Fe^{2+} and Fe^{4+} are generated, respectively. The Fe^{2+} could be oxidized to Fe^{3+} by transferring electrons to absorbed O_2 on the surface of TiO_2 (Eq. (5)) or to a neighboring surface Ti^{4+} (Eq. (6)), thereby leading to interfacial electron transfer (Eq. (7)). The trapped holes in Fe^{4+} could migrate to surface

adsorbed hydroxyl ions (Eq. (8)) to produce hydroxyl radicals. As a result, the introduction of Fe ions reduces electron–hole recombination rate and improves the photoactivity:[5]

$$Fe^{3+} + h^+ \rightarrow Fe^{4+} \quad (3)$$

$$Fe^{3+} + e^- \rightarrow Fe^{2+} \quad (4)$$

$$Fe^{2+} + O_2(ads) \rightarrow Fe^{3+} + HO_2^- \quad (5)$$

$$Fe^{2+} + Ti^{4+} \rightarrow Fe^{3+} + Ti^{3+} \quad (6)$$

$$Ti^{3+} + O_2(ads) \rightarrow Ti^{4+} + HO_2^- \quad (7)$$

$$Fe^{4+} + OH^- (ads) \rightarrow Fe^{3+} + {}^{\bullet}OH(ads) \quad (8)$$

As can be seen in Fig. 5, the presence of H_2O_2 increased the photocatalytic efficiency of the TiO_2, which could be explained by the electron-acceptor role of H_2O_2. With the 3.4Fe/TiO_2 catalyst, the presence of H_2O_2 increased the efficiency to a high extent. This means that H_2O_2 in addition to its electron-acceptor role also participates in the heterogeneous photo-Fenton process.

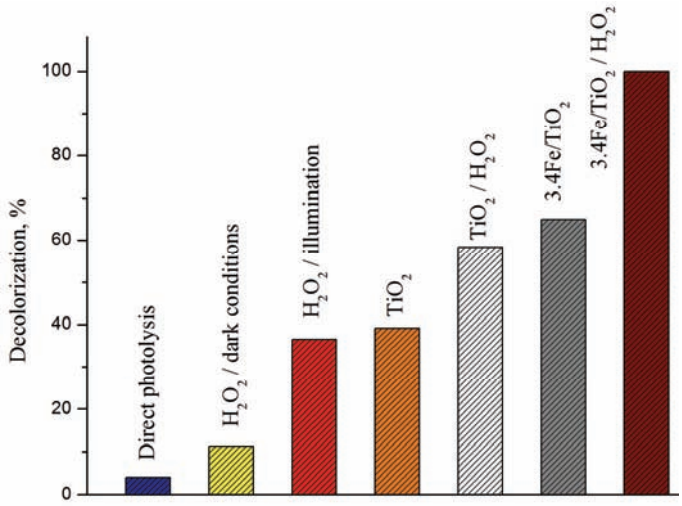

Fig. 5. Decolorization of RB using different AOPs. Operating conditions: $[RB]_0$ = 60 mg dm^{-3}, $[H_2O_2]_0$ = 20 mM, photocatalysts, 0.5 g dm^{-3}, pH 4 and time = 60 min.

Effect of Fe content

The influence of the doping concentration on the photocatalytic efficiency of the Fenton-like process was examined and the results are presented in Fig. 6. It could be seen that the optimal amount of Fe doping was 3.4 %, as this level of doping led to the complete elimination of RB within 60 min. Hence, all the other investigations were performed using the 3.4Fe/TiO_2 catalyst. It could be noticed that a further increase in the Fe content led to a decrease in the photoactivity. An explanation about the beneficial effect of Fe ions was given above. Thus, Fe^{3+}

act as both electron and hole traps, but they can also act as recombination centers for photogenerated electrons. When the dopant concentration is too high, the recombination will compete with the redox processes because the distance between trap sites is shorter. These trapped e^- or h^+ might recombine before migrating to the surface, resulting in a lower photocatalytic activity, because all the reactions occur only on the surface.[30]

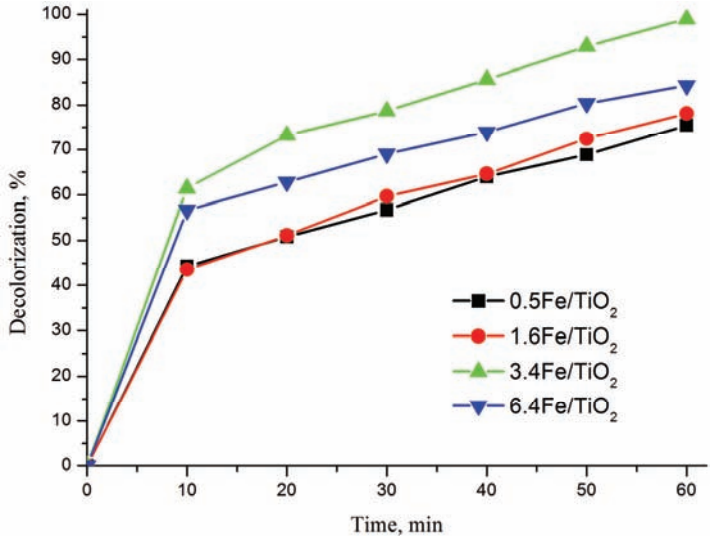

Fig. 6. Effect of Fe content in Fe/TiO_2 on the RB decolorization. Operating conditions: $[RB]_0$ = 60 mg dm^{-3} $[H_2O_2]_0$ = 20 mM, photocatalysts, 0.5 g dm^{-3} and pH 4.

The adsorption properties of Fe/TiO_2 catalysts are shown in Fig. 7. The adsorption capacity of the powders increased with increasing Fe ion doping. The factors leading to the enhanced adsorption capacity involve changes in the physical properties owing to doping. In the present case, it was the larger specific surface area that enabled better adsorption of RB. Thus, the largest specific surface area and the highest content of Fe ions with H_2O_2 in Fenton-like process gave reasons to expect that the $6.4Fe/TiO_2$ catalyst would be the most efficient. Figures 6 and 7 illustrate that the photocatalytic activity did not follow the changes of the adsorption ability. Although adsorption is a prerequisite for the photocatalytic process, it is not obligatory that large adsorption abilities stimulate a faster degradation of the pollutant. An increase in photoactivity with increasing adsorption could be observed up to a certain amount of dopant but a decrease thereafter. This indicates that some other factors influence the degradation efficiency, *i.e.*, at higher contents, Fe^{3+} play the role of recombination sites and this effect dominates.

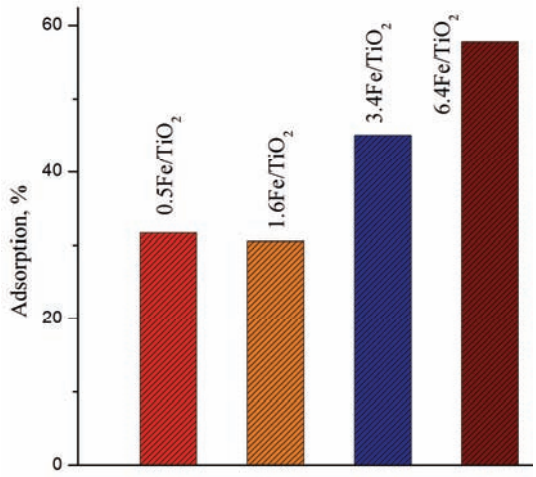

Fig. 7. Sorption ability of the Fe/TiO_2 catalysts. Operating conditions: $[RB]_0$ = 60 mg dm^{-3}, photocatalysts, 0.5 g dm^{-3}, pH 4 and time = 60 min.

Effect of the initial pH

The pH plays an important role in the photocatalytic degradation of various pollutants.[31,32] The effect of pH on the kinetics of RB removal by the 3.4Fe/TiO_2 photocatalyst is presented in Fig. 8, which clearly indicates that the pH value had a great effect on the photocatalytic efficiency. It could be seen that the efficiency decreased with increasing pH value. This could be explained by the fact that the higher values of pH favor the dissociation of H_2O_2 to form HO_2^-, as shown in Eq. (9):

$$H_2O_2 \rightleftharpoons HO_2^- + H^+ \quad (9)$$

HO_2^- reacts with a non-dissociated molecule of H_2O_2 according to Eq. (10), which leads to oxygen and water, instead of hydroxyl radicals.

$$HO_2^- + H_2O_2 \rightarrow H_2O + O_2 + OH^- \quad (10)$$

At pH > 7, the ionic dissociation of H_2O_2 is the predominant process, hence, no experiments under alkaline conditions were performed.[33] In addition, a possible cause of such behavior could be the fact that the oxidation potential of $^{\bullet}OH$ decreases with increasing pH.[34]

The best results were obtained at a pH value of 3. The inset of Fig. 8 shows the leaching of iron after the photocatalytic process. The leaching of Fe ions was enhanced at pH 3; hence, in this case, the homogeneous photo-Fenton process contributed to the overall photodegradation. Since the efficiency was the same after 60 min at pH 4, only with different kinetics, and the detected concentration of Fe ions was only 24 μg dm^{-3}, this pH value was chosen as the optimum for the further experiments. Fe leaching to such a low extent does not have a significant influence on the photodegradation.

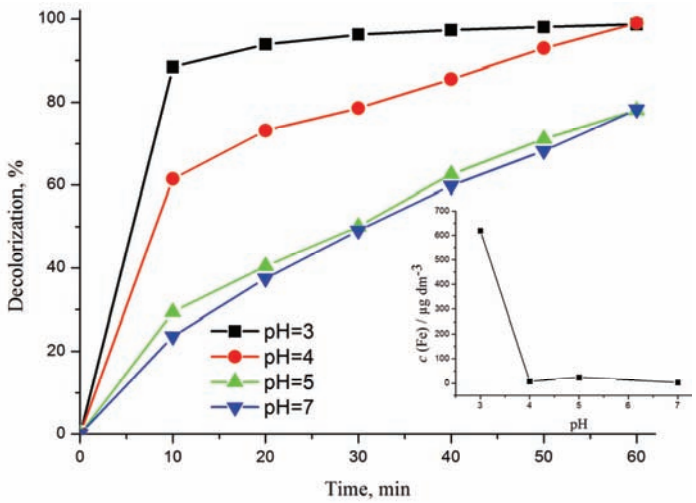

Fig. 8. Effect of solution pH on the RB decolorization in the presence of 3.4Fe/TiO_2. The inset shows the effect of the initial pH on the leaching of iron. Operating conditions: $[RB]_0$ = 60 mg dm^{-3} $[H_2O_2]_0$ = 20 mM and photocatalyst, 0.5 g dm^{-3}.

One additional possible reason of such dependence on the pH value is the influence of adsorption and the results are presented in Fig. 9. A strong electrostatic attraction between dye and the surface exists when the Fe/TiO_2 surface is positively charged and the dye is negatively charged. At lower pH values, the conditions for sorption were optimal.

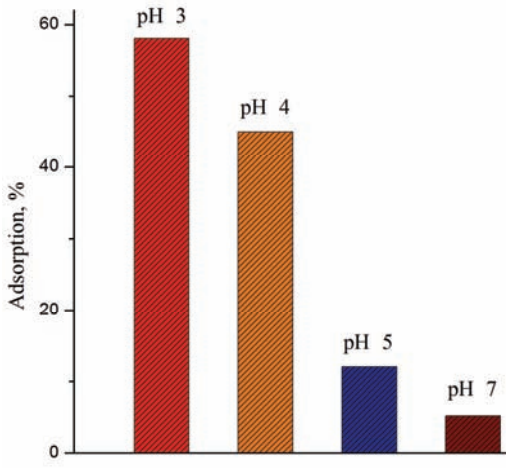

Fig. 9. Sorption ability of the 3.4Fe//TiO_2 catalyst at different pH values. Operating conditions: $[RB]_0$ = 60 mg dm^{-3}, photocatalyst, 0.5 g dm^{-3} and time = 60 min.

Degradation of a colorless pollutant

When the compound used as model pollutant absorbs in the visible region, such as the azo dye in the present study, the dye rather than the TiO_2 particles is

excited by visible light. After excitation, the electrons from the dye molecule are injected into the TiO_2 conduction band. The TiO_2 acts only as an electron transfer mediator in this reaction.[35] Thus, an experiment with 4-CP was performed to prove that the studied catalyst is capable of degrading colorless pollutants and to produce reactive oxygen species, meaning that excitation of the dye molecule is not the only mechanism. The results are shown in Fig. 10, from which it can be seen that after just 10 min of the treatment, the 4-CP peak with a retention time of about 10 min had almost disappeared. Three additional peaks of degradation products with retention times of 6.8, 2.9 and 1 min appeared. In Fig. 10c, after 20 min of the treatment, a further decrease in the intensity of the peaks, indicating further degradation, could be observed.

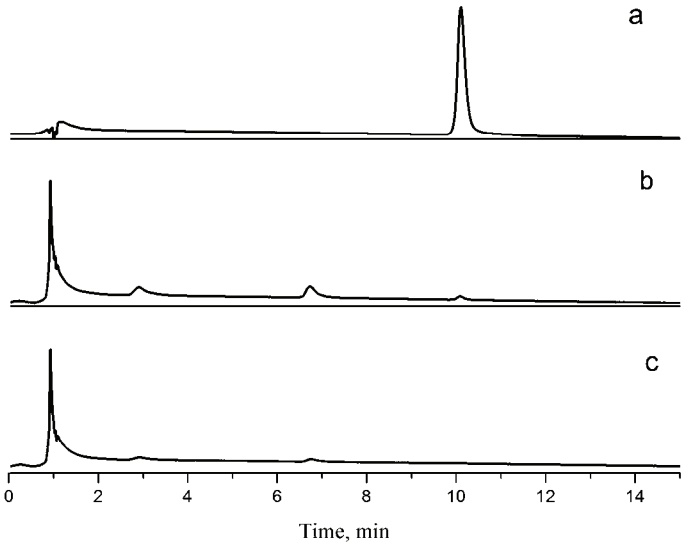

Fig. 10. Chromatograms of 4-CP degraded by the 3.4Fe/TiO_2 catalyst at different times: a) 0; b) 10 and c) 20 min. Operating conditions: $[4\text{-CP}]_0$ = 100 mg dm^{-3}, $[H_2O_2]_0$ = 20 mM, photocatalyst, 0.5 g dm^{-3} and pH 4.

CONCLUSIONS

Fe/TiO_2 photocatalysts with different contents of Fe (0.5, 1.6, 3.4 and 6.4 %) were successfully prepared by the microwave-hydrothermal method. The XRD results showed that the Fe^{3+} were highly dispersed in the TiO_2 lattice. The Fe doping influenced the textural characteristics of the synthesized photocatalysts, increasing the specific surface area, which is the critical parameter for the enhancement of photocatalytic activity. Furthermore, Fe doping played a role in extending the light absorption into the visible region. Fe–TiO_2 can efficiently catalyze the degradation of RB under sun-like irradiation in the presence of H_2O_2. The photocatalyst 3.4Fe/TiO_2 was found to be the most efficient with

H_2O_2. The results indicate that the pH value had a great effect on the photocatalytic efficiency. The decolorization of RB by the 3.4Fe/TiO_2/H_2O_2 process was more favorable at acidic pH values. With pH > 4, the release of Fe ions into the solution was negligible in the heterogeneous photo-Fenton process.

Under the optimal experimental conditions, the catalyst was able to degrade even a colorless pollutant. Therefore, it could be considered a good candidate for wastewaters remediation purposes.

Acknowledgements. This work is supported by the Ministry of Education, Science and Technological Development of the Republic of Serbia (Contracts No. 172030 and 172035).

И З В О Д

ФЕНТОНОВА ОКСИДАЦИЈА АЗО БОЈЕ ПОМОЋУ МЕЗОПОРОЗНОГ Fe/TiO_2 ПРИПРЕМЉЕНОГ ХИДРОТЕРМАЛНОМ МЕТОДОМ ПОТПОМОГНУТОМ МИКРОТАЛАСИМА

ЈЕЛЕНА НЕШИЋ[1], ДРАГАН Д. МАНОЈЛОВИЋ[2], МИЛИЦА ЈОВИЋ[1], БИЉАНА П. ДОЈЧИНОВИЋ[3], ПРЕДРАГ Ј. ВУЛИЋ[4], ЈУГОСЛАВ КРСТИЋ[5] и ГОРАН М. РОГЛИЋ[2]

[1]Иновациони центар Хемијског факултета, Универзитет у Београду, Студентски трг 12, 11000 Београд, [2]Хемијски факултет, Универзитет у Београду, Студентски трг 12, 11000 Београд, [3]Институт за хемију, технологију и металургију, Центар за хемију, Универзитет у Београду, Његошева 12, 11000 Београд, [4]Лабораторија за кристалографију, Рударско–геолошки факултет, Универзитет у Београду, Ђушина 7, 11000 Београд и [5]Институт за хемију, технологију и металургију, Центар за катализу и хемијско инжењерство, Универзитет у Београду, Његошева 12, 11000 Београд

Fe-допирани TiO_2 фотокатализатори са различитим садржајем гвожђа (0,5, 1,6, 3,4 и 6,4 %) синтетисани су микроталасно–хидротермалном методом и карактерисани помоћу XRD, физисорпције N_2 на 77 K и DRS методом. Карактеризација је показала да су јони гвожђа потпуно дисперговани унутар кристалне решетке TiO_2. Нађено је да сви катализатори имају мезопорозну структуру и да Fe-допирање повећава специфичну површину. UV–Vis спектри показују да се апсорпција помера ка већим таласним дужинама (црвено померање) са повећањем концентрације допанта. Фотокаталитичка активност узорака је процењена на основу деколоризације текстилне реактивне боје реактивно плаво 52 (RB) у воденом раствору помоћу лампе са спектром сунчевог зрачења у присуству H_2O_2 (хетерогени фото-Фентонов процес). Фотокатализатор са 3,4 % гвожђа се показао као најефикаснији са H_2O_2. Утицај иницијалне pH вредности је утврђен и испитано је отпуштање јона гвожђа у зависности од pH. Закључено је да је погоднија кисела средина за деколоризацију и да је, када је pH > 4, отпуштање гвожђа у раствор занемарљиво. Испитана је фотокаталитичка деградација 4-хлорфенола (4-CP) при оптималним условима и показало се да је дати катализатор способан и за деградације безбојних загађивача.

(Примљено 1. октобра, ревидирано 20 новембра, прихваћено 21. новембра 2013)

REFERENCES

1. M. A. Behnajady, N. Modirshahla, H. Fathi, *J. Hazard. Mater*., *B* **136** (2006) 816
2. O. Lergini, E. Oliveros, A. M. Braun, *Chem. Rev.* **93** (1993) 671
3. M. S. Lucas, J. A. *Dyes Pigm.* **74** (2007) 622

4. V. Augugliaro, V. Loddo, G. Palmisano, L. Palmisano, *Clean by light irradiation: Practical applications of supported TiO_2*, The Royal Society of Chemistry, Cambridge, UK, 2010, p. 15
5. J. Zhu, F. Chen, J. Zhang, H. Chen, M. Anpo, *J. Photochem. Photobiol., A* **180** (2006) 196
6. M. Zhou, J. Yu, B. Cheng, H. Yu, *Mater. Chem. Phys.* **93** (2005) 159
7. X. H. Wang, J.-G. Li, H. Kamiyama, Y. Moriyoshi, T. Ishigaki, *J. Phys. Chem., B* **110** (2006) 6804
8. J. A. Rengifo-Herrera, E. Mielczarski, J. Mielczarski, N. C. Castillo, J. Kiwi, C. Pulgarin, *Appl. Catal., B* **84** (2008) 448
9. A. Dobosz, A. Sobczynski, *Water Res.* **37** (2003) 1489
10. Z. Xiong, J. Ma, W. J. Ng, T. D. Waite, X. S. Zhao, *Water Res.* **45** (2011) 2095
11. C. Fountzoula, N. Spanos, H. K. Matralis, C. Kordulis, *Appl. Catal., B* **35** (2002) 295
12. J. Nešić, D. D. Manojlović, I. Anđelković, B. P. Dojčinović, P. J. Vulić, J. Krstić, G. M. Roglić, *J. Mol. Catal., A* **378** (2013) 67
13. F. Mazille, T. Schoettl, C. Pulgarin, *Appl. Catal., B* **89** (2009) 635
14. F. Mazille , A. Lopez, C. Pulgarin, *Appl. Catal., B* **90** (2009) 321
15. N. Banić, B. Abramović, J. Krstic, D. Šojic, D. Lončarević, Z. Cherkezova-Zheleva, V. Guzsvany, *Appl. Catal., B* **107** (2011) 363
16. J. Rodríguez-Carvajal, *FullProf Suite: Crystallographic tools for Rietveld, profile matching & integrated intensity refinements of X-ray and/or neutron data*. http://www.ill.eu/ /sites/fullprof/
17. S. Brunauer, P. H. Emmett, E. Teller, *J. Am. Chem. Soc.* **60** (1938) 309
18. S. J. Gregg, K. S. W. Sing, *Adsorption, Surface Area and Porosity*, Academic Press, London, 1982, p. 126
19. F. Rouquerol, J. Rouquerol, K. Sing, *Adsorption by powders and porous solids*, Academic Press, London, 1999, p. 111
20. E. P. Barrett, L. G. Joyner, P. P. Halenda, *J. Am. Chem. Soc.* **73** (1951) 373
21. J. Chen, M. Yao, X. Wang, *J. Nanopart. Res.* **10** (2008) 163
22. Y. C. Cao, T. He, Y. Chen, Y. Cao, *J. Phys. Chem., C* **114** (2010) 3627
23. Y. Wang, H. Cheng, Y. Hao, J. Ma, W. Li, S. Cai, *J. Mater. Sci.* **34** (1999) 3721
24. J. Rouquerol , D. Avnir, C. W. Fairbridge, D. H. Everett, J. H. Haynes, N. Pemicone, J. D. F. Ramsay, K. S. W. Sing, K. K. Unger, *Pure Appl. Chem.* **66** (1994) 1739
25. T. Umebayashi, T. Yamaki, H. Itoh, K. Asail, *J. Phys. Chem. Solids* **63** (2002) 1909
26. J. Zhu, W. Zheng, B. He, J. Zhang, M. Anpo, *J. Mol. Catal., A* **216** (2004) 35
27. Y. Jiaguo, X. Quanjun, Z. Minghua, *Appl. Catal., B* **90** (2009) 595
28. J. Mitrović, M. Radović, D. Bojić, T. Anđelković, M. Purenović, A. Bojić, *J. Serb. Chem. Soc.* **77** (2012) 465
29. T. Tong, J. Zhang, B. Tian, F. Chen, D. He, *J. Hazard. Mater*. **155** (2008) 572
30. B. Zhao, G. Mele, I. Pio, J. Li, L. Palmisano, G. Vasapollo, *J. Hazard. Mater*. **176** (2010) 569
31. C. Lizama, J. Freer, J. Baeza, H. D. Mansilla, *Catal. Today* **76** (2002) 235
32. S. Sakthivel, B. Neppolian, M. V. Shankar, B. Arabindoo, M. Palanichamy, V. Murugesan, *Sol. Energy Mater. Sol. Cells* **77** (2003) 65
33. M. I. Stefan, A. R. Hoy, J. R. Bolton, *Environ. Sci. Technol.* **30** (1996) 2382
34. H. R. Eisenhauer, *J.-Water Pollut. Control Fed.* **36** (1964) 1116
35. M. A. Fox, M. T. Dulay, *Chem. Rev.* **93** (1993) 341.